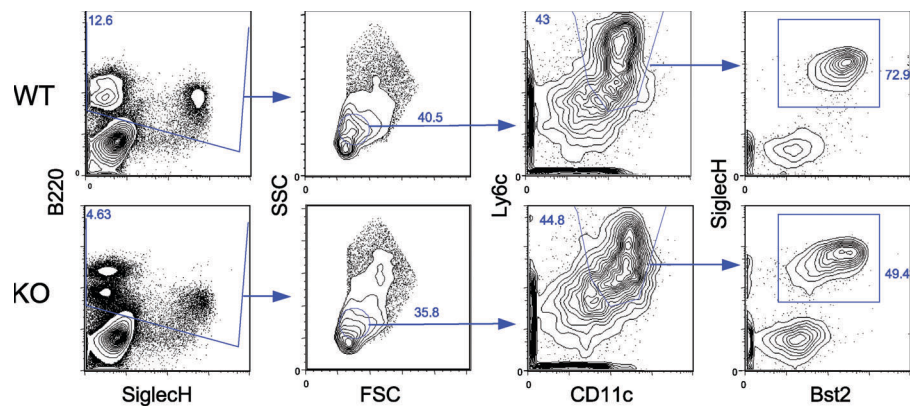
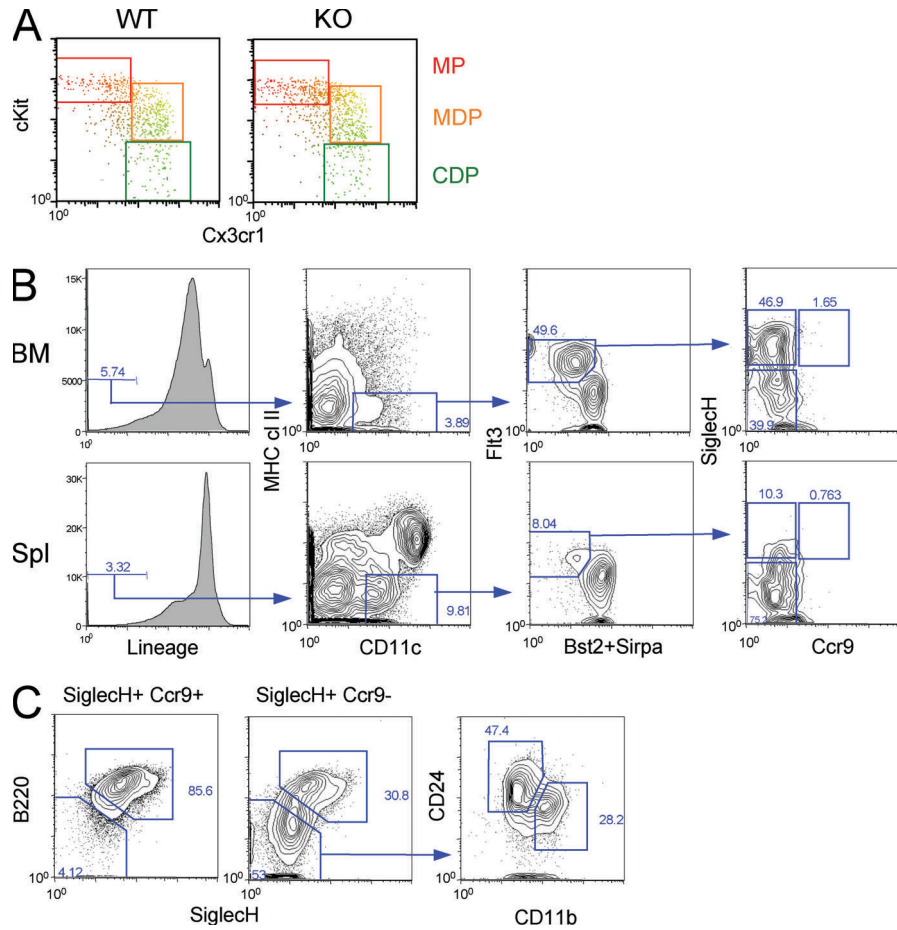


SUPPLEMENTAL MATERIAL

Ghosh et al., <http://www.jem.org/cgi/content/full/jem.20132121/DC1>



**Figure S1.** A representative gating strategy to define pDCs in the BM of Mtg16-deficient mice. Note the combination of multiple broad gates that accommodate lower expression levels of some markers (B220, Ly6C, and Bst2); also note that other markers (e.g., CD11c and SiglecH) are unaffected in Mtg16-null pDCs.



**Figure S2. Characterization of DC progenitors.** (A) Phenotypic definition of  $\text{Lin}^- \text{Sca1}^- \text{Flt3}^+$  progenitors in the BM of WT and  $\text{Mtg16}^{-/-}$  (KO) mice. MDP, monocyte/DC progenitor. (B) Gating strategy to define subsets of pre-DCs in the BM of WT mice. (C) The progeny of  $\text{SiglecH}^+$  pre-DC subsets that were sorted and cultured with Flt3L. Note that the  $\text{SiglecH}^+ \text{Ccr9}^+$  subset produced exclusively pDCs, whereas the  $\text{SiglecH}^+ \text{Ccr9}^-$  subset gave rise to pDCs and two cDC subsets.

Dataset S1, included as a separate Excel file, shows genome-wide expression analysis of  $\text{Mtg16}^{-/-}$  pDCs.

Dataset S2, included as a separate Excel file, shows ChIP-Seq results for MTG16 and E2-2 in CAL-1 cells.